Genome-Wide Computational Analysis of Dioxin Response Element Location and Distribution in the Human, Mouse, and Rat Genomes

ARTICLE *in* CHEMICAL RESEARCH IN TOXICOLOGY · MARCH 2011

Impact Factor: 3.53 · DOI: 10.1021/tx100328r · Source: PubMed

4 AUTHORS, INCLUDING:

Edward Dere
Brown University
19 PUBLICATIONS **328** CITATIONS
SEE PROFILE

Lyle D Burgoon
Engineer Research and Development Center …
65 PUBLICATIONS **1,641** CITATIONS
SEE PROFILE

Chemical Research in Toxicology

ARTICLE

pubs.acs.org/crt

Genome-Wide Computational Analysis of Dioxin Response Element Location and Distribution in the Human, Mouse, and Rat Genomes

Edward Dere,[†] Agnes L. Forgacs,[†,‡] Timothy R. Zacharewski,[*,†,‡,§] and Lyle D. Burgoon[†,‡,§,∥]

[†]Department of Biochemistry & Molecular Biology, [‡]Center for Integrative Toxicology, [§]Gene Expression in Development and Disease Initiative, and [∥]Quantitative Biology Initiative, Michigan State University, East Lansing, Michigan 48824, United States

Supporting Information

ABSTRACT: The aryl hydrocarbon receptor (AhR) mediates responses elicited by 2,3,7,8-tetrachlorodibenzo-*p*-dioxin by binding to dioxin response elements (DRE) containing the core consensus sequence 5′-GCGTG-3′. The human, mouse, and rat genomes were computationally searched for all DRE cores. Each core was then extended by 7 bp upstream and downstream, and matrix similarity (MS) scores for the resulting 19 bp DRE sequences were calculated using a revised position weight matrix constructed from bona fide functional DREs. In total, 72318 human, 70720 mouse, and 88651 rat high-scoring (MS ≥ 0.8437) putative DREs were identified. Gene-encoding intragenic DNA regions had ∼1.6 times more putative DREs than the noncoding intergenic DNA regions. Furthermore, the promoter region spanning ±1.5 kb of a TSS had the highest density of putative DREs within the genome. Chromosomal analysis found that the putative DRE densities of chromosomes X and Y were significantly lower than the mean chromosomal density. Interestingly, the 10 kb upstream promoter region on chromosome X of the genomes were significantly less dense than the chromosomal mean, while the same region in chromosome Y was the most dense. In addition to providing a detailed genomic map of all DRE cores in the human, mouse, and rat genomes, these data will further aid the elucidation of AhR-mediated signal transduction.

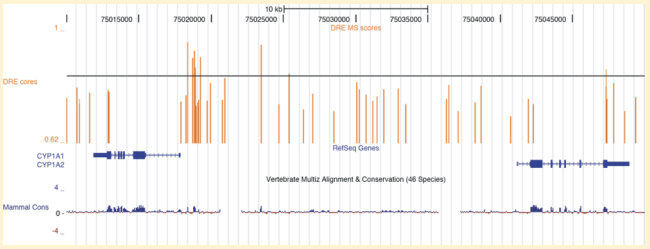

INTRODUCTION

cis-Regulatory elements located in the promoter region of genes are transcription factor binding sites that regulate gene expression. Most transcription factors have a preferred response element sequence to which they bind. The identification and location of these elements are important in elucidating transcription factor binding, signal transduction, and, ultimately, their gene expression networks. Binding to elements in the proximal promoter region stabilizes the general transcriptional machinery at the transcriptional start site (TSS) to regulate gene expression. However, global location analyses of transcription factor binding using ChIP-chip and ChIP-seq technologies have demonstrated transcription factor binding at sites distant from the TSS.[1−4] A comprehensive map of transcription factor binding element locations and distribution within a genome provides important complementary information for elucidating and modeling the gene expression network of a transcription factor.

The AhR is a ligand-activated transcription factor belonging to the basic helix−loop−helix PAS (bHLH-PAS) family of proteins that serve as environmental sensors to different stimuli.[5] 2,3,7,8-Tetrachlorodibenzo-*p*-dioxin (TCDD) is the prototypical ligand, a widespread environmental contaminant that elicits diverse species-specific effects, including tumor promotion, teratogenesis, hepatotoxicity, modulation of endocrine systems, immunotoxicity, and enzyme induction.[6,7] These effects are a result of changes in gene expression mediated by the AhR.[8] The binding of TCDD and related compounds to the cytosolic AhR triggers a conformational change and translocation of the activated receptor to the nucleus where it heterodimerizes with the aryl hydrocarbon nuclear translocator (ARNT), another bHLH-PAS family member. The heterodimer then binds to dioxin response elements (DREs) containing the 5′-GCGTG-3′ core, to regulate gene expression.[8,9] Evidence indicates that nucleotides adjacent to the core consensus sequence modulate DNA-binding affinity and enhancer function.[10−12]

Position weight matrices (PWMs) provide a similarity assessment of a motif or putative response element.[13] When compared to a consensus sequence, they have been used to rank and prioritize potential transcription factor binding site preferences. However, PWMs suffer from high false positive prediction rates since the probability of any nucleotide at any position within the binding site is assumed to be independent of all other positions. Fortunately, the DRE PWM is based on the 5′-GCGTG-3′ core, thus reducing false positive frequency.[14]

We have previously identified the location and distribution of DREs relative to the TSS for a limited number of genes[14] based on prior builds of the human, mouse, and rat genome assemblies.[14] Improvements and innovations in sequencing technologies have

Received: September 21, 2010
Published: March 03, 2011

Table 1. Bona Fide DRE Sequences Used To Construct the Revised[a] PWM

species	gene symbol	RefSeq identifier	position relative to TSS	bona fide DRE sequence[b]	matrix similarity score	reference
mouse	Cyp1a1	NM_001136059	−491	caagctc**GCGTG**agaagcg	0.9466	11
	Cyp1a1	NM_001136059	−871	cctgtgt**GCGTG**ccaagca	0.9128	11
	Cyp1a1	NM_001136059	−984	cggagtt**GCGTG**agaagag	0.9598	11
	Cyp1a1	NM_001136059	−1059	ccagcta**GCGTG**acagcac	0.9260	11
	Cyp1a1	NM_001136059	−1206	cgggttt**GCGTG**cgatgct	0.9610	11
	Cyp1b1	NM_009994	−872	ccccctt**GCGTG**cggagct	0.9514	23
rat	Cyp1a1	NM_012540	−1045	cggagtt**GCGTG**agaagag	0.9598	20
	Cyp1a1	NM_012540	−1120	ccagcta**GCGTG**acagcac	0.9260	20
	Aldh3a1	NM_031972	−6787	tgccctg**GCGTG**actttgt[c]	0.8473[d]	24
	Nqo1	NM_017000	−400	tcccctt**GCGTG**caaaggc	0.9332	19
	Sod1	NM_017050	−274	gaggcct**GCGTG**cgcgcct	0.8481	22
	Gsta2[e]	NM_017013	−910	gcatgtt**GCGTG**catccct	0.8728	21
	Ugt1a6[e]	NM_057105	−3856	agaatgt**GCGTG**acaaggt	0.8950	18

[a] Bona fide DRE sequences were updated using mm9 and rn4 genome builds. [b] Sequences used in Sun et al.[14] were updated with the mm9 and rn4 genome builds; revised sequences are underlined. [c] Replaces previous DRE sequence for ratAldh3a1. [d] Denotes the MS score used as the threshold score. [e] Gsta2 and Ugt1a6 were previously named GstYa and Ugt1a1, respectively, and were renamed within the rn4 genome build.

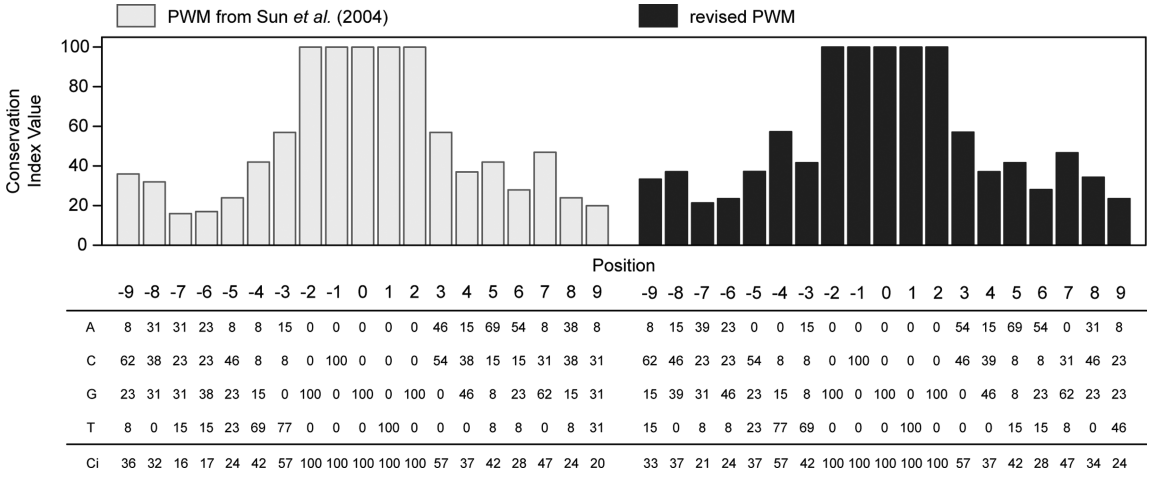

Figure 1. Comparison of the previously published PWM and conservation index (C_i) for DREs with the revised PWM. The matrix and plot of the C_i on the left (light gray bars) was previously published by Sun et al.[14] The matrix and plot (black) on the right is the revised PWM and C_i using the current mouse (mm9) and rat (rn4) genome assemblies from the UCSC Genome Browser. The matrix (bottom) shows the percentage of occurrence for a specific nucleotide at that given position. For example, positions −2 to 2 define the 5′-GCGTG-3′ DRE core, and each nucleotide within the core has a C_i value of 100. The histogram (top) is a graphical representation of the C_i values, which are listed below the PWM. The C_i provides a measure of conservation at each base pair position. If a PWM is 100% conserved at a position, the C_i value is 100, whereas if the position is truly random (A = 25%, C = 25%, G = 25%, and T = 25%), then the C_i value is 0.

since provided higher quality data with significantly fewer sequence gaps[15−17] in the most recent genome builds resulting in more accurate annotation. In addition, the latest mouse and rat genome builds were used to construct a revised PWM based on updated sequence information for 13 bona fide functional DREs. Consequently, we have expanded the scope of our initial DRE analysis to include the entire human, mouse, and rat genomes using an improved PWM. This includes analyses of the intragenic (10 kb upstream to end of 3′ UTR) and intergenic DNA regions and chromosome and gene regions [10 kb upstream of a TSS, 5′ and 3′ untranslated regions (UTRs), and coding sequence (CDS)]. Collectively, these results provide a detailed genomic map for all putative DREs in the human, mouse, and rat genomes that will serve as an important resource for the further elucidation of AhR gene expression networks.

EXPERIMENTAL PROCEDURES

PWM. We have previously constructed a PWM using 13 bona fide functional DRE sequences from previous assembly builds of the mouse (mm3) and rat (rn2) genomes.[11,14,18−23] These sequences were updated using the sequence information from the current genome assemblies for the mouse (mm9) and rat (rn4) (Table 1, updated sequences are underlined). Additionally, the previously identified sequence for the bona fide rat *Aldh3a1* DRE could no longer be found in the rn4 genome build and was replaced with a functional DRE located 6 787 bp upstream of the TSS.[24] Also note that the gene names for *GstYa* and *Ugt1a1* have changed to *Gsta2* and *Ugt1a6*, respectively, in the latest rat assembly. Updated sequences were used to develop a revised *PWM* using the bona fide 19 bp DRE-centered sequences (Figure 1). The replaced rat Aldh3a1 DRE sequence had the lowest matrix similarity

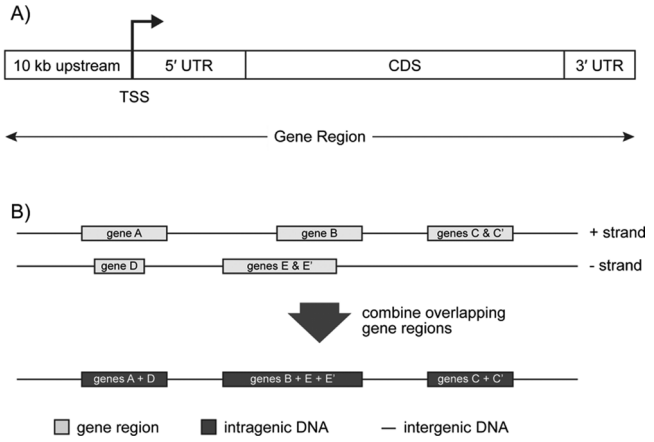

Figure 2. Defining the various genomic regions used for DRE location analysis. (A) Genomic locations from the UCSC Genome Browser refGene database were used to obtain sequences for 10 kb region upstream of the TSS, the 5′ and 3′ UTRs, and the CDS of every known human, mouse, and rat RefSeq sequence. A gene region is defined as the sequence spanning the region 10 kb upstream of a TSS through to the end of the 3′ UTR. (B) Intragenic DNA regions in a genome were determined by combining the nonoverlapping gene regions. For example, gene regions of tissue specific isoforms of a gene that have different TSS positions were merged to determine the longest spanning range (genes C and C′ and genes E and E′). Additionally, overlapping genes on both strands of the genome were also merged (genes B + E + E′). Nontranscribed DNA segments that span the regions between adjacent intragenic regions are defined as the intergenic DNA regions.

(MS) score (0.8473), which was subsequently used as a threshold value to define 19 bp DRE sequences as putative DREs that were functional.

Whole-Genome Identification of DREs. Sequences for human (hg19), mouse (mm9), and rat (rn4) genome assemblies and associated annotation within the refGene and refLink databases were downloaded from the UCSC Genome Browser.[25] Individual segments of a gene region (i.e., the 10 kb sequence upstream of a TSS, the 5′ and 3′ UTRs, and the CDS) for each mature gene-encoding reference sequence (RefSeqs with NM prefixed identifiers) were determined using the genomic coordinates within the refGene databases (Figure 2A). Intragenic DNA regions within the genomes were computationally identified by merging overlapping gene regions (defined in Figure 2A) from both strands of the genome, and the DNA between adjacent intragenic regions is defined as the nontranscribed intergenic DNA regions (Figure 2B). The lengths for each of these defined regions and the number of RefSeqs on each chromosome are provided for the human, mouse, and rat genomes in the Supporting Information (Table 1). In total, 28 906 human, 24 327 mouse, and 15 737 rat mature RefSeqs were searched. Gene annotation associated with each RefSeq sequence was derived from the refLink database in the UCSC Genome Browser.

The sequence of each individual chromosome was computationally searched for the 5′-GCGTG-3′ core sequence using a previously described search algorithm.[14] Each core was then extended by 7 bp upstream and downstream of the core. MS scores for the 19 bp DRE sequences were calculated using the revised PWM. For genomic location analysis, the position of a DRE core is defined as the center base (5′-GCGTG-3′) of the 5 bp core sequence (underlined). Putative DRE densities were calculated based on the number of putative DREs occurring in an interrogated region (e.g., intergenic DNA region or 5′ UTR) divided by the total sum of the region length. Results from the computational genome-wide DRE search can be downloaded as bedGraph track format (Supporting Information, files 5−7) and uploaded to the UCSC Genome Browser for visualization (Figure 3).

Putative DRE densities from the different defined genomic regions (i.e., intergenic, intragenic, 10 kb upstream, UTRs, and CDS) were identified as non-Gaussian using Q−Q plots (car package; qq.plot). The Wilcoxon rank sum test (nonparametric t test) was used to compare intergenic and intragenic putative DRE densities within species. The Kruskal−Wallis test (nonparametric one-way ANOVA), followed by the Nemenyi−Demico−Wolfe−Dunn Test (nonparametric Tukey's test; nemenyi.test.R) was used to compare the putative DRE densities in the 10 kb upstream, 5′ UTR, CDS, and 3′ UTR DRE densities within species. All analyses were performed in R (version 2.12.0).

Random Sequence Comparison. To investigate the random frequency of DRE cores within each genome, 25 000 random sequences of 15 kb in length were computationally generated by randomly selecting A, C, G, or Ts. These sequences were then searched for DRE cores, and the 19 bp DRE sequence MS score was calculated using the described algorithm[14] with the revised PWM.

Microarray Analysis. Whole-genome microarray analysis of hepatic tissue from mice orally gavaged with 30 μg/kg TCDD was performed using 4 × 44k whole genome oligonucleotide arrays from Agilent Technologies (Santa Clara, CA). The same RNA from a previous study was used for the gene expression profiling.[26] Changes in gene expression due to TCDD treatment were conducted according to the manufacturer's Two-Color Microarray-Based Gene Expression Analysis protocol Version 5.0.1. Microarray data were normalized using a semiparametric method[27] and statistically analyzed using an empirical Bayes method.[28] Differentially expressed genes were determined by both a fold change and a statistical cutoff ($|\text{fold change}| \geq 1.5$ and $P1(t) \geq 0.999$).

RESULTS

PWM. Our previous PWM used bona fide DRE sequence information from earlier drafts of the mouse (mm3) and rat (rn2) genomes (Figure 1). These sequences have since been updated with the most current information available from the mouse (mm9) and rat (rn4) genome assemblies (Table 1). As a result, the sequence of two bona fide DREs in the promoter region of the mouse and rat *Cyp1a1* gene have changed (Table 1, see footnote b). Additionally, the previously used DRE for rat *Aldh3a1* could no longer be found in the latest rat genomic sequence and was replaced with a recently characterized DRE located 6.8 kb upstream of the TSS[24] (Table 1). These updates altered the PWM and the conservation index (C_i) vector, which represents the degree of conservation of the individual nucleotide position, primarily in the 7 bp flanking 5′ arm of the consensus sequence (Figure 1). Recalculation of MS scores for the bona fide DREs identified the rat *Aldh3a1* motif as having the lowest score, 0.8473, which was subsequently used to characterize computationally identified sequences as putative DREs.

Genome-Wide Distribution of DREs. Our previous computational search for the 5′-GCGTG-3′ DRE core was limited to sequences 5 kb upstream and 2 kb downstream of a TSS for known RefSeqs in previous genome builds.[14] This current study extended the search to the entire human, mouse, and rat genomes, including the nontranscribed intergenic DNA regions (Figure 2B). Computational searches identified 1.65, 1.04, and 1.07 million DRE cores in the human, mouse, and rat genomes, respectively (Table 2). After extending these cores by the 7 bp upstream and downstream flanking sequences, MS scores were calculated using the revised PWM. A total of 72 318 human, 70 720 mouse, and 88 651 rat 19 bp DRE sequences had a MS score greater than or equal to 0.8473 and were classified as putatively functional DREs (Table 2). The densities of putative DREs with respect to the

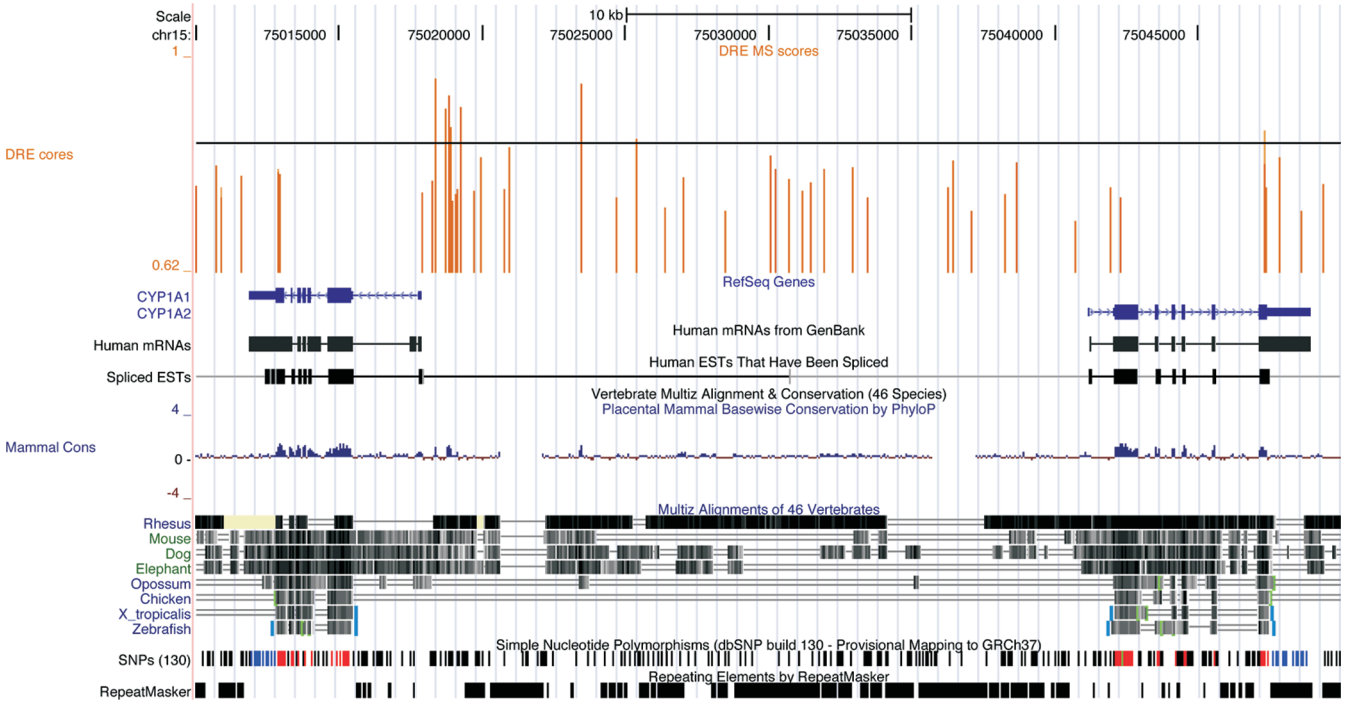

Figure 3. Visualization of DRE sequence locations in the UCSC Genome Browser for human CYP1A1 and CYP1A2 gene regions and adjacent intergenic regions. The genomic location and MS score for each identified 19 bp DRE sequence have been loaded into the UCSC Genome Browser as a bedGraph track (see DRE cores track at top). The vertical bars represent the 5 bp DRE core, and the height of the bar provides an indication of the MS score for the 19 bp DRE core-containing sequence. The horizontal black line within the DRE cores track indicates the threshold MS score (0.8473) to assist with the identification of putative functional DREs.

Table 2. Distribution of DRE Cores, Putative DREs, and Putative DRE Densities across the Human, Mouse, and Rat Genomes

					gene region[b]			
	species	genome	intergenic DNA[a]	intragenic DNA[a]	10kb upstream[c]	5′ UTR[c]	CDS[c]	3′ UTR[c]
region length (Mbp[d])	human	3 096	1 836	1 260	295	236	1 599	44
	mouse	2 655	1 588	1 067	247	149	1 040	31
	rat	2 719	1 973	746	159	74	569	18
total number of DRE cores	human	1 648 651	759 030	889 621	303 016	172 235	1 054 383	26 925
	mouse	1 036 996	492 703	544 293	154 921	82 306	510 060	16 546
	rat	1 070 366	676 193	394 173	94 514	41 455	292 526	9 711
total number of putative DREs[e]	human	72 318	34 322	37 996	13 272	7 606	46 004	1 123
	mouse	70 720	33 018	37 702	10 176	6 024	35 819	1 220
	rat	88 651	54 888	33 763	7 962	3 515	24 954	870
putative DRE density (per Mbp[d])	human	23.4	18.7	30.2	45.0	32.2	28.8	25.6
	mouse	26.6	20.8	35.3	41.3	40.5	34.5	39.5
	rat	32.6	27.8	45.3	50.2	47.6	43.9	49.4

[a] Intergenic and intragenic DNA region are defined in Figure 2B. [b] The gene region is defined as the transcribed gene plus 10 kb usptream of the TSS as depicted in Figure 2A. [c] Regions are defined using the genomic locations in the refGene database from the UCSC Genome Browser. [d] Mbp = million basepairs. [e] Putative DREs defined as the 19 bp DRE centered core-containing sequence with a MS score ≥0.8473.

total length of the genomes were 23.4, 26.6, and 32.6 DREs per million base pairs (Mbp) in the human, mouse, and rat, respectively. These values were determined from searching 3.10 billion human, 2.66 billion mouse, and 2.72 billion rat base pairs (Table 2).

Approximately 40% of the human, 40% of the mouse, and 27% of the rat genomes are comprised of intragenic DNA (Figure 2B); 53% of all putative DREs in the human and mouse genomes were identified in these regions, while only 38% of all putative DREs mapped to the intragenic DNA in the rat (Table 2). This difference is likely a result of the relatively fewer number of rat RefSeqs (15 737) as compared to the human (28 906) and the mouse (24 327). Relative putative DRE densities (i.e., intragenic/intergenic DNA putative density ratio) suggest that intragenic regions have ~1.6 times greater putative DRE density as compared to intergenic DNA regions in each genome. For

dx.doi.org/10.1021/tx100328r |Chem. Res. Toxicol. 2011, 24, 494–504

Table 3. Chromosomal Density of Putative DREs[a] (Per Mbp[b]) within the Intergenic and Intragenic DNA Regions[c] of the Human, Mouse, and Rat Genomes

	human			mouse			rat		
chromosome	total	intergenic DNA	intragenic DNA	total	intergenic DNA	intragenic DNA	total	intergenic DNA	intragenic DNA
1	22.7	17.5	28.9	24.0	20.1	30.1[d]	32.9	28.4	42.3
2	22.9	20.0	27.0[d]	28.2	23.3	33.9	26.5[d]	23.0[d]	38.8[d]
3	19.8[d]	16.1[d]	24.2[d]	23.7	18.7	33.9	35.2	31.1	43.9
4	19.3[d]	17.2	23.1[d]	28.8	21.5	39.5[e]	30.1	26.1	39.1[d]
5	21.0	19.0	24.4[d]	32.3[e]	24.3[e]	42.4[e]	31.6	26.9	45.4
6	20.9	18.8	23.9[d]	26.2	21.2	32.8	32.8	28.2	46.2
7	25.3	20.7	30.6	26.7	19.7	36.7	34.8	29.2	49.2
8	24.3	21.6	28.6	29.6	23.2	39.9[e]	36.1	30.9	47.5
9	22.0	16.7[d]	31.3	30.1	23.9[e]	36.9	33.5	30.1	42.8
10	26.4	22.9[e]	30.5	28.6	22.1	37.6	43.8[e]	37.4[e]	53.9[e]
11	24.7	18.9	31.2	33.9[e]	26.7[e]	40.9[e]	29.6	24.4[d]	44.0
12	24.0	20.0	28.5	27.0	22.3	35.7	62.7[e]	52.0[e]	81.3[e]
13	16.7[d]	13.4[d]	25.3[d]	26.6	23.7[e]	31.6	31.3	26.4	44.0
14	19.9[d]	15.1[d]	28.9	24.8	21.0	31.1	32.4	29.0	43.1
15	23.2	18.6	30.1	26.7	19.3	37.8	29.8	26.1	41.2
16	35.0[e]	25.6[e]	48.0[e]	24.6	19.4	32.9	33.3	27.6	48.3
17	34.8[e]	26.6[e]	40.7[e]	31.0[e]	22.7	40.9[e]	36.1	33.6	43.1
18	23.3	19.6	29.8	26.7	20.2	37.7	30.7	26.7	43.3
19	43.6[e]	29.7[e]	53.3	30.8[e]	23.2	38.4	43.2[e]	38.6[e]	53.5
20	32.5[e]	27.0[e]	38.7[e]				45.0[e]	34.4[e]	68.5[e]
21	23.0	15.6[d]	44.2[e]						
22	33.3[e]	21.5	51.5[e]						
X	19.4[d]	16.9	24.7[d]	12.6[d]	11.1[d]	16.4[d]	16.0[d]	14.5[d]	25.5[d]
Y[f]	9.5[d]	8.1[d]	27.9	4.5[d]	3.7[d]	16.4[d]			
mean density	24.5	19.5	32.3	26.1	20.5	34.5	34.6	29.8	46.9
SD	7.1	4.7	8.9	6.5	4.9	6.9	8.9	7.2	11.1

[a] Putative DREs defined as the 19 bp DRE centered core-containing sequence with a MS score ≥0.8473. [b] Mbp = million basepairs. [c] Intergenic and intragenic DNA region are defined in Figure 2B. [d] Putative DRE density is less than the lower limit of the 99% confidence interval of the mean. [e] Putative DRE density is greater than the upper limit of the 99% confidence interval of the mean. [f] No sequence data for chromosome Y is available in rn4 build of the rat genome.

example, the human genome had putative DRE densities per Mbp of 30.2 and 18.7 in the intragenic and intergenic DNA regions, respectively (30.2/18.7 = 1.6). This suggests that there is a greater likelihood of putative DREs in the intragenic regions of the genome as opposed to the nontranscribed intergenic DNA regions. However, the density of putative DREs was generally higher in the rat genome (Table 2), likely due to the relative immaturity of gene annotation associated with the rat genome. The location and MS score for each identified 19 bp DRE sequence have been loaded into the UCSC Genome browser and can be visualized as a bedGraph track (Figure 3). The nonparametric Wilcoxon rank sum test of the mean chromosomal intragenic and intergenic putative DRE densities for each species (Table 3) identified significant intragenic enrichment with respect to the intergenic DNA regions. Further examination of DRE distribution within defined gene region segments (i.e., 10 kb upstream, 5′ and 3′ UTRs, and CDS; Figure 2A) found that segment-specific putative DREs densities were comparable in human and mouse regions. Kruskal−Wallis nonparametric tests of the mean chromosomal putative DRE densities (Table 4) confirmed significantly higher density of putative DREs in the 10 kb upstream and 5′ UTR relative to the CDS in the human and mouse genomes. Although these same regions in the rat genome possessed a higher density of putative DREs relative to the CDS, statistical analyses were not able to detect any significant differences in the densities.

Chromosome Level Analysis of Putative DREs. To further investigate putative DRE distribution across the genomes, chromosomal level analysis was performed (Tables 3 and 4). Examination of individual chromosomes identified examples where the putative DRE density was significantly different than the mean chromosomal value (outside the 99% confidence interval of the mean; Table 3, see footnotes d and e). For example, putative DRE densities for rat chromosome 2 and human chromosome 13 were 26.5 and 16.7 per Mbp, respectively, which were significantly less than the mean value for each genome (34.6 and 24.5 per Mbp, for the rat and human, respectively). Furthermore, human chromosomes 16 and 17 had significantly greater putative DREs density than the mean chromosomal density. There are also instances where the putative DRE densities in the intergenic DNA (Table 3), or in a specific gene region segment (i.e., 10 kb upstream region, CDS and UTRs; Table 4), were significantly different than the chromosomal mean for that region. These data suggest that there are chromosome- and segment-specific biases

Table 4. Chromosomal Density of Putative DREs[a] (Per Mbp[b]) within the 10 kb Upstream, 5′ and 3′ UTRs, and CDS Regions[c] of RefSeq Sequences in the Human, Mouse, and Rat Genomes

	human				mouse				rat			
chromosome	10 kb upstream	5′ UTR	CDS	3′ UTR	10 kb upstream	5′ UTR	CDS	3′ UTR	10 kb upstream	5′ UTR	CDS	3′ UTR
1	35.8[d]	27.5	27.3	22.1[d]	39.8	30.6[d]	29.6	32.8	43.3[d]	52.6	41.7	34.6[d]
2	62.2[e]	40.2	27.1	26.2	38.8	41.2	34.0	36.1	49.7	34.9[d]	37.1[d]	36.2[d]
3	51.4	18.1[d]	22.9[d]	24.8	41.9	42.6	31.2	40.3	48.4	33.6[d]	44.0	61.9
4	57.4[e]	29.2	28.6	27.5	49.4[e]	46.1	37.2	43.1	42.6[d]	36.1[d]	38.2	42.9[d]
5	54.0	43.8	28.9	30.4	49.1[e]	58.7[e]	38.8[e]	34.0	53.7	53.4	43.5	50.8
6	41.4	28.4	26.8	23.8	35.0[d]	37.7	32.4	38.5	49.2	54.6	44.7	39.1[d]
7	49.9	32.5	27.2	30.4	36.5	41.6	39.1[e]	44.9	60.2[e]	49.9	49.0	51.8
8	52.2	27.6	27.0[d]	29.7	48.7[e]	33.6[d]	39.6[e]	50.4[e]	50.5	49.1	45.2	50.4
9	46.1	28.9	30.3	35.1[e]	40.2	42.9	36.4	44.8	47.4	51.5	41.2	66.4[e]
10	50.8	29.4	23.2	24.5	40.3	33.6[d]	34.2	40.1	54.3	66.4[e]	51.6	48.7
11	34.9[d]	37.4	27.7	24.4	48.2[e]	52.0[e]	39.5[e]	47.2[e]	48.8	33.9[d]	44.8	77.6[e]
12	42.4	27.4	26.0[d]	16.4[d]	42.3	38.5	36.4	50.9[e]	77.7	69.1[e]	84.5[e]	61.1
13	84.8[e]	47.6[e]	31..8	48.1[e]	34.0[d]	36.2	30.3	37.6	42.5[d]	54.6	42.6	55.2
14	56.7[e]	32.7	26.2[d]	30.2	40.6	40.7	31.7	40.6	42.0[d]	55.3	42.3	67.1[e]
15	47.0	27.0[d]	34.1	27.3	48.4[e]	41.9	39.1[e]	41.4	46.5	42.7[d]	39.3	73.3[e]
16	51.6	41.3	49.4[e]	47.9[e]	39.8	40.9	29.9	41.3	65.1	63.3[e]	43.9	65.9[e]
17	33.8[d]	60.5[e]	31.5	18.2[d]	46.4[e]	46.4	41.9[e]	39.8	46.3	53.8	41.5	37.4[d]
18	76.0[e]	30.1	35.7	35.1[e]	40.4	38.3	37.8	37.0	53.8	48.8	39.3	25.2[d]
19	25.0[d]	50.9[e]	52.7[e]	27.6	43.0	51.3[e]	37.3	38.4	55.4	48.9	52.4	58.1
20	49.9	33.7	37.0[e]	20.7[d]					64.0[e]	58.9[e]	73.7[e]	78.3[e]
21	41.6	19.2[d]	32.5	21.7[d]								
22	42.9	51.4[e]	41.3[e]	28.3								
X	26.8[d]	25.0[d]	21.4[d]	12.9[d]	20.5[d]	19.8[d]	14.8[d]	14.5[d]	31.0[d]	30.3[d]	23.2[d]	34.4[d]
Y[f]	45.2	98.9[e]	42.6[e]	16.7[d]	26.7[d]	84.1[e]	13.3[d]	0.0[d]				
mean density	48.3	37.0	31.6	27.1	40.5	42.8	33.5	37.8	51.1	49.6	45.9	53.2
SD	13.6	16.8	8.0	8.5	7.3	12.5	7.4	11.4	9.9	10.9	12.6	15.3

[a] Putative DREs defined as the 19 bp DRE centered core-containing sequence with a MS score ≥0.8473. [b] Mbp = million basepairs. [c] Regions are defined using the genomic locations in the refGene database from the UCSC Genome Browser. [d] Putative DRE density is less than the lower limit of the 99% confidence interval of the mean. [e] Putative DRE density is greater than the upper limit of the 99% confidence interval of the mean. [f] No sequence data for chromosome Y is available in m4 build of the rat genome.

in putative DRE densities across the genome that may have biological relevance in AhR-mediated responses.

Interestingly, putative DRE densities in chromosome X and Y of the human and mouse were significantly lower than the chromosomal average (Tables 3 and 4; there currently is no sequence data available for chromosome Y in the rat). For example, mouse chromosome Y has an intragenic putative DRE density of 16.4 per Mbp, almost half the density of any other mouse chromosome for the same region. In contrast, the putative density in the 5′ UTR for chromosome Y was 84.1 per Mbp, nearly double the chromosomal average in the mouse genome. Human chromosome Y was similar with a lower putative DRE density in the intragenic region, but the 5′ UTR density was more than 2.6 times greater than the mean chromosomal value. Similar to chromosome Y, the putative densities in the intragenic regions of chromosome X were significantly lower than the mean in each genome. However, unlike chromosome Y, the density in the 5′ UTR was also lower than the mean chromosome value. Such region differences in chromosomes X and Y may contribute to sex-specific AhR-mediated responses. It is important to recognize that the lower total putative DRE densities in the sex chromosomes are likely due to the lower chromosomal contribution of intragenic DNA. For example, intragenic DNA accounts for only 6% of the total DNA on human chromosome Y as compared to 36% on human chromosome 9. Supporting Information Tables 2 and 3 provide a complete chromosomal summary of the total number of putative DRE in the intergenic and intragenic DNA regions, the UTRs, and the CDS for the human, mouse, and rat genomes.

Random Sequence Analysis. To examine the chance occurrence of putative DREs, 25 000 random sequences of 15 kb were generated and searched for DREs. The computational search found 731 636 core sequences and, extending these sequences by 7 bp on both ends, identified 108 210 chance occurrences of putative DREs (MS score ≥ 0.8473). In total, 375 Mbp were searched resulting in 288.6 putative DREs per Mbp. This chance occurrence of putative DRE density is significantly greater than the calculated densities in each genome at both the global and the chromosomal level, suggesting that regions with a high density of putative DREs have a greater likelihood of being biologically significant.

Putative DRE Density Proximal to the TSS. Putative DRE densities across genomes and chromosomes provide a gross estimate of occurrence. Finer analysis of different gene region

dx.doi.org/10.1021/tx100328r |Chem. Res. Toxicol. 2011, 24, 494–504

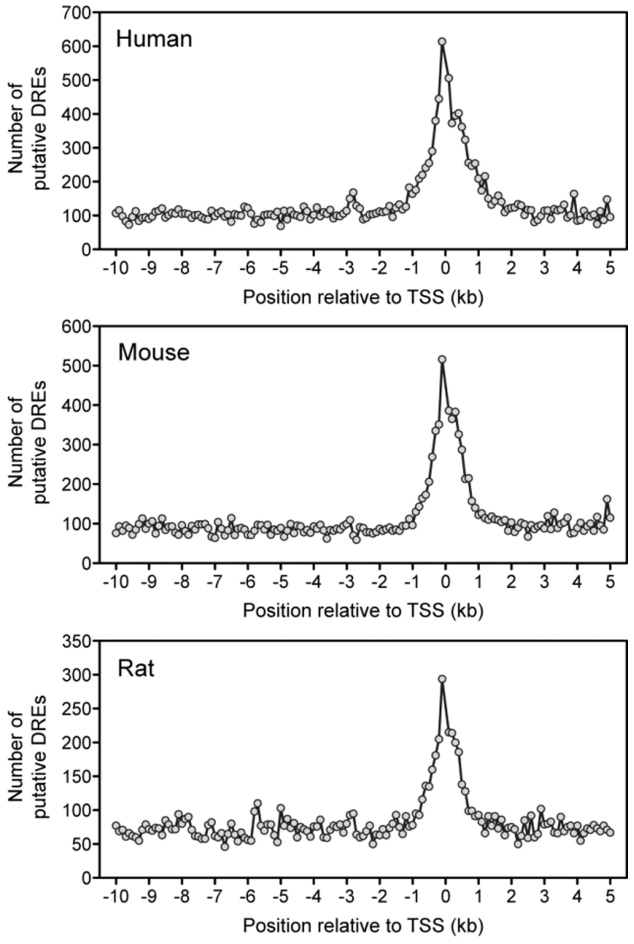

Figure 4. Distribution of putative DREs in the regions 10 kb upstream to 5 kb downstream of a TSS for all RefSeq sequences. The −10 to 5 kb region of a TSS were divided into nonoverlapping 100 bp windows. The total number of putative DREs (MS score ≥0.8473) was determined for each 100 bp window and graphed. The density of putative DREs was greatest in the 3 kb region centered around the TSS.

segments generally found greater putative DRE density in the 10 kb upstream and 5′ UTR regions. To further investigate these segments, the number of putative DREs in nonoverlapping 100 bp windows spanning the region 10 kb upstream and 5 kb downstream of a TSS was plotted (Figure 4). Putative DREs were not equally distributed within this 15 kb region, with the highest density occurring within ±1.5 kb of a TSS. In each species, the density was the greatest at approximately 100 bp directly upstream of the TSS. A sharp 3′ drop from the maximum was observed followed by a secondary peak 200−400 bp downstream of the TSS before putative DRE occurrence returned to basal levels.

Gene Level Analysis of DREs. Unique Entrez Gene identifiers for mature gene-encoding RefSeqs (NM prefixed RefSeq identifiers) were obtained from the UCSC Genome Browser refLink database and used to determine the distribution of putative DREs associated with 18 893 human, 20 018 mouse, and 15 342 rat annotated genes (Table 5). The majority of all known genes had at least one DRE core present within 10 kb upstream of the TSS and the transcribed gene. However, 55 human, 343 mouse, and 327 rat genes did not have a DRE core within this same region. It is surprising to identify so many genes without a

Table 5. Analysis of DRE Core and Putative DRE Containing RefSeq Sequences and Genes in the Human, Mouse, and Rat Genomes

	human		mouse		rat	
	RefSeqs	genes	RefSeqs	genes	RefSeqs	genes
genome[a]	28 906	18 893	24 327	20 018	15 737	15 342
with a DRE core	28 871	18 858	23 982	19 675	15 409	15 015
with a putative DRE[b]	20 502	13 050	15 885	12 628	10 105	9 809

[a] Based on RefSeqs and Entrez Gene IDs stored in the refGene and refLink databases from the UCSC Genome Browser. [b] Pulative DREs defined as the 19 bp DRE centered core-containing sequence with a MS score ≥0.8473.

DRE core since the average gene region length (10 kb upstream of a TSS plus the transcribed gene) in the different genomes is 61 kb and the 5′-GCGTG-3′ sequence is expected to occur once every 512 bp. The lack of a DRE core in these genes may suggest that they are not targets of AhR regulation. However, 7 of the 343 mouse genes without a DRE core were differentially regulated in the temporal microarray data set. These responses may be regulated by AhR-independent mechanisms or via distally located DREs. Subsequent statistical analysis using a χ^2 test resulted in a p value <0.001 ($\alpha = 0.05$), illustrating a significant difference in the number of genes with and without a DRE core. Although there are a significant number of genes not containing a DRE core within the region 10 kb upstream of a TSS plus the transcribed gene, distal DREs in the intragenic DNA regions may also have functional importance, consistent with reported DRE-independent AhR mediated gene expression.[29]

Further restricting this analysis to the 19 bp DRE sequences with a MS score ≥ 0.8473 (i.e., putative DREs) identified 69, 63, and 64% of all human, mouse, and rat genes, respectively, had at least one putative DRE (Table 5). Moreover, approximately 60% of all human, mouse, and rat genes have 1−10 putative DREs (Figure 5). Interestingly, the maximum number of putative DREs was found in human *PTPRN2* with 134, mouse *Wwox* with 73, and rat *Odz2* with 65. Orthologues of these genes also had a high number of putative DREs. For example, there were 24 and 25 putative DREs in the mouse and rat *PTPRN2*, respectively. However, neither gene has been explicitly investigated for their responsiveness to TCDD nor are these genes responsive in our or any other TCDD microarray data sets.[30−34] Unfortunately, the global gene expression effects of TCDD have been investigated in a limited number of models (e.g., in vitro and in vivo human, mouse, and rat hepatic tissue, human breast cancer cells, and mouse uterus). Gene expression is species-, sex-, age-, tissue-, and cell-specific; therefore, the effects of TCDD on *PTPRN2*, *Wwox*, and *Odz2* gene expression warrant further investigation in other models to determine their potential AhR regulation.

Global hepatic temporal gene expression analysis at 2, 4, 8, 12, 18, 24, 72, and 168 h identified 1 896 genes that were differentially expressed (|fold change| ≥ 1.5 and P1(t) ≥ 0.999) at one or more time points following a single oral dose of 30 μg/kg TCDD in immature, ovariectomized C57BL/6 mice. Of these, 1 247 had putative DREs within the 10 kb upstream or transcribed regions (includes 5′ and 3′ UTR and CDS). Genes that exhibited significant differential expression in the mouse liver included *Fabp12* with 8 putative DREs (23.5-fold induction) and *Cyp1a1* with 7 putative DREs (205-fold induction). The remaining 649

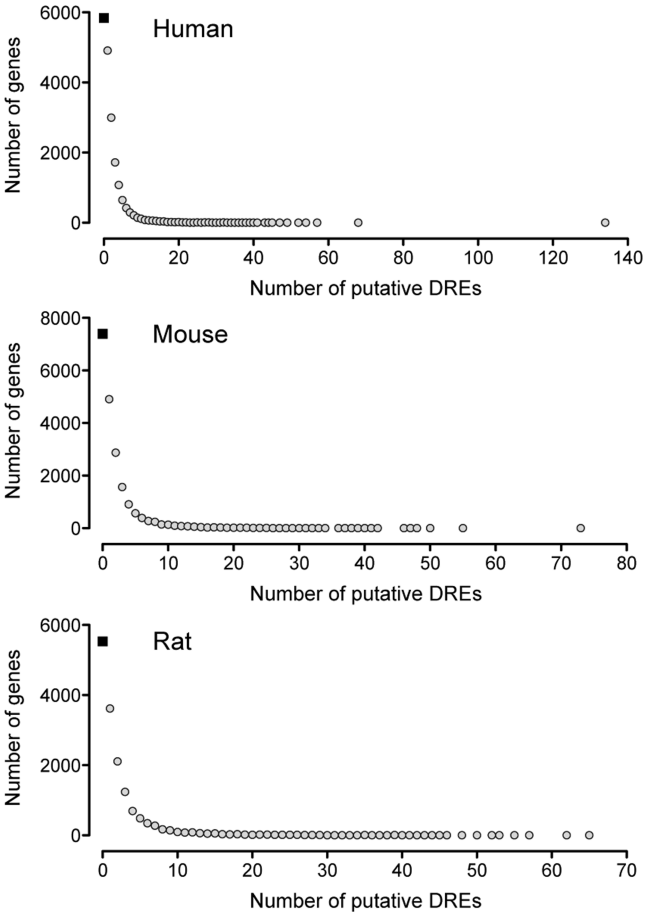

Figure 5. Frequency of putative DREs within known human, mouse, and rat genes. For each species, the gene region (10 kb upstream of a TSS through to the end of the 3′ UTR) was searched for putative DREs. Approximately 35% of all known genes did not contain a putative DRE (black box), while nearly 60% of all genes had between 1 and 10 putative DREs. Approximately 5% of all genes have more than 10 putative DREs.

differentially expressed genes, which included unannotated and hypothetical genes, did not have a putative DRE. Examining only well-annotated genes found 593 TCDD responsive genes without a putative DRE within the region 10 kb upstream or transcribed region. The responses of some these genes include the up-regulation of Chad (+6.88-fold) and Olfr114 (+9.97-fold) and the repression of *Serpina7* (−7.98-fold). The complete microarray data set is available in the Supporting Information (Table 4). The responses of *Olfr114* and *Serpina7* have previously been reported to be AhR-dependent;[35−37] however, it is unclear if the responses of these genes are directly mediated by the activated AhR complex or secondary responses.

Differentially regulated genes indentified through microarray analysis of TCDD-treated immature, ovariectomized Sprague−Dawley rats[31,32] were also searched for putative DREs. From those studies, 604 genes were responsive ($|\text{fold change}| \geq 1.5$ and $P1(t) \geq 0.99$) at 2 or more time points and 528 had at least one putative DRE within the 10 kb upstream or transcribed regions. This current mouse microarray study and the previous rat studies covered 5 451 orthologous genes, and only 52 of those were responsive in both models and possessed at least one putative DRE. These results are consistent with our previous orthologous promoter analysis that demonstrated that few human, mouse, and rat orthologues had positionally conserved DRE upstream of a TSS.[14]

DISCUSSION

Genome-wide identification of potential cis-acting regulatory elements provides important information for elucidating signaling networks. Many computational and traditional in vitro approaches have generally focused on relatively few genes and a small segment of a target gene promoter, while neglecting more distal elements, which may also have important regulatory roles.[14,38−43] To fully elucidate the signaling transduction of transcription factors, both proximally and distally located response elements need to be identified and characterized.

The structure and function of the AhR as well as its mode of action are highly conserved, with homologues found in nearly all vertebrates. AhR activation by TCDD results in target gene expression via the DRE core sequence, 5′-GCGTG-3′. Our previous DRE computational analysis was limited to the proximal promoter regions (5 kb upstream to 2 kb downstream of a TSS) of known genes in earlier drafts of the human, mouse, and rat genomes.[14] This current study leverages the availability of higher quality finished human and mouse assemblies,[15,44] as well as the most current build of the rat genome to establish a revised PWM and calculate MS scores for all DRE core-containing sequences located throughout the human, mouse, and rat genomes, including the nontranscribed intragenic DNA regions.

Approximately 60% of the human and mouse genomes consist of stretches of nontranscribed intergenic DNA, while we define the remaining 40% as intragenic regions that include the 10 kb upstream promoter region, the 5′ and 3′ UTRs, and the CDS (Table 2). Despite these differences in length, the total number of DRE core sequences and putative DREs were comparable in the intergenic DNA and intragenic regions. The draft assembly of the rat genome consists predominantly of intergenic DNA (73%), reflecting the immaturity of its annotation. Consequently, the intergenic DNA bias in the rat resulted in a greater number of identified DRE cores and putative DREs in the intergenic DNA regions as compared to intragenic DNA. Even within intragenic regions, putative DREs were found in CDS and 3′ UTR regions and not limited to proximal-promoters (Table 4).

It has been suggested that the relative location of a bound transcription factor may have different roles in regulating gene expression. For example, the estrogen receptor (ER), p53, and forkhead box protein A1[1−4] interact with proximal and distal response elements located throughout the genome, including the intergenic DNA. Transcription factor binding at the core promoter is presumed to stabilize the basal transcriptional machinery, while more distal motifs exert regulation through a looping mechanism or by altering chromatin structure.[45−47] Consequently, a comprehensive map of potential binding sites throughout the genome provides important information for elucidating the AhR gene expression network.

Computational searches identified putative DREs in all genome regions. However, once the size of each region was taken into consideration, the density of putative DREs was found to be highest in the intragenic DNA regions of all three species. Moreover, putative DRE densities varied dramatically across chromosomes with some chromosomes having significantly higher densities (e.g., human chromosome 19, mouse chromosome 5, and rat chromosome 12) as compared to the mean chromosomal density, while others (e.g., human chromosome 13 and chromosome rat 2)

were significantly less dense. Interestingly, the sex chromosomes, and especially chromosome Y, the rat genome withstanding, were the least dense in terms of the total putative DREs among all of the other chromosomes. Putative DRE densities within the 10 kb upstream region, the UTRs, and the CDS were also substantially different from the mean chromosomal value for those regions. TCDD elicits sex-specific physiological and gene expression responses in rodents.[7,48,49] These differences in sensitivity and physiological responses may be influenced by DREs differentially regulating gene expression on the sex chromosomes. Note that no sequence information for chromosome Y is currently available in the rat draft assembly. This will likely be resolved in the next phase of the rat genome sequencing effort.[16,50]

Within human and mouse chromosomes, putative DRE densities were highest in the 5′ UTR and the region 10 kb upstream of the TSS. In contrast, DRE densities in rat genes were slightly higher in the 3′ UTR as compared to either the 10 kb upstream region or the 5′ UTR. However, as previously mentioned, limited annotation of the rat genome may have biased the identification of DREs to the 3′ UTR. A more finite analysis of the density around the proximal promoter found the greatest putative DRE density within ±1.5 kb of the TSS of known RefSeq sequences for all three species, with the maximum density occurring 100 bp upstream of a TSS. This coincides with 70% of all RNA polymerase II (Pol II) binding,[2,3] suggesting that proximal AhR binding recruits and stabilizes Pol II binding at the TSS. Additionally, because of the GC rich nature of the DRE core sequence, the putative DRE density profile mirrors the CpG island frequency in the proximal promoter region.[51] Consequently, the methylation status of putative DRE cores within CpG islands may affect gene expression. However, in a recent study, inhibition of DNA methylation by AzaC in human MCF-7 cells did not affect TCDD-induced *CYP1A1* expression.[52]

Searching the region 10 kb upstream of a TSS and the transcribed region for all known genes in the genomes found that approximately 65% of all genes contained at least one putative DRE. However, gene expression is species-, sex-, age-, tissue-, cell-, and promoter context-dependent. Moreover, many responses may be secondary, thereby not involving direct interaction with the AhR. Consequently, the presence of a putative DRE within the gene region is not sufficient to elicit a transcriptional response. Although our use of a MS score ≥ 0.8473 to define a 19 bp DRE sequence as putative is based on experimental data, indicating that it is the lowest scoring bona fide functional DRE (i.e., rat *Aldh3a1* DRE), recent protein-binding microarray studies indicate that more degenerative sites also bind transcription factors and have important functional roles in regulating gene expression.[53,54]

Transcription factors can also indirectly regulate gene expression by tethering to other proximally bound transcription factors. For example, progesterone receptor tethers to Sp1, Stat5, and AP1 to regulate genes independent of a progesterone response element.[55−57] Moreover, the AhR is recruited to estrogen-responsive regions in a gene-specific[58] and DRE-independent manner.[59] Furthermore, AhR:ARNT heterodimers regulate target gene expression by interacting with an alternate response element sequence, independent of the DRE core consensus sequence.[60,61] All of these factors must be taken into context to fully comprehend AhR-mediated gene regulation.

Computationally searching the human, mouse, and rat genome assemblies has revealed that putative DREs are not randomly distributed. Our detailed genomic map has identified putative DREs in intergenic and intragenic DNA regions. Furthermore, putative DRE distributions vary across specific genome regions. This suggests that AhR binding to putative DREs in different genomic locations may have differing roles in regulating gene expression. Complementary studies are in progress to investigate AhR complex binding to DREs located in intergenic and intragenic regions.

■ ASSOCIATED CONTENT

Supporting Information. Tables of numbers of distinct gene encoding RefSeqs in the human, mouse, and rat genomes by chromosome; chromosomal distribution of putative DREs within the intergenic and intragenic DNA regions of the human, mouse, and rat genomes; chromosomal distribution of putative DREs within the 10 kb upstream, 5′ and 3′ UTRs, and CDS regions of RefSeq sequences in the human, mouse, and rat genomes; and C57BL/6 mice TCDD temporal microarray data. This material is available free of charge via the Internet at http://pubs.acs.org.

■ AUTHOR INFORMATION

Corresponding Author

*Tel: 517-355-1607. Fax: 517-432-2310. E-mail: tzachare@msu.edu.

Funding Sources

This work was supported by the National Institute of Environmental Health Sciences Superfund Basic Research Program (P42ES04911).

■ ACKNOWLEDGMENT

We thank Dr. Jason Matthews for critically reviewing this manuscript.

■ REFERENCES

(1) Carroll, J. S., Liu, X. S., Brodsky, A. S., Li, W., Meyer, C. A., Szary, A. J., Eeckhoute, J., Shao, W., Hestermann, E. V., Geistlinger, T. R., Fox, E. A., Silver, P. A., and Brown, M. (2005) Chromosome-wide mapping of estrogen receptor binding reveals long-range regulation requiring the forkhead protein FoxA1. *Cell 122*, 33–43.

(2) Carroll, J. S., Meyer, C. A., Song, J., Li, W., Geistlinger, T. R., Eeckhoute, J., Brodsky, A. S., Keeton, E. K., Fertuck, K. C., Hall, G. F., Wang, Q., Bekiranov, S., Sementchenko, V., Fox, E. A., Silver, P. A., Gingeras, T. R., Liu, X. S., and Brown, M. (2006) Genome-wide analysis of estrogen receptor binding sites. *Nat. Genet. 38*, 1289–1297.

(3) Lin, C.-Y., Vega, V. B., Thomsen, J. S., Zhang, T., Kong, S. L., Xie, M., Chiu, K. P., Lipovich, L., Barnett, D. H., Stossi, F., Yeo, A., George, J., Kuznetsov, V. A., Lee, Y. K., Charn, T. H., Palanisamy, N., Miller, L. D., Cheung, E., Katzenellenbogen, B. S., Ruan, Y., Bourque, G., Wei, C.-L., and Liu, E. T. (2007) Whole-genome cartography of estrogen receptor alpha binding sites. *PLoS Genet. 3*, e87.

(4) Wederell, E. D., Bilenky, M., Cullum, R., Thiessen, N., Dagpinar, M., Delaney, A., Varhol, R., Zhao, Y., Zeng, T., Bernier, B., Ingham, M., Hirst, M., Robertson, G., Marra, M. A., Jones, S., and Hoodless, P. A. (2008) Global analysis of in vivo Foxa2-binding sites in mouse adult liver using massively parallel sequencing. *Nucleic Acids Res. 36*, 4549–4564.

(5) Gu, Y., Hogenesch, J., and Bradfield, C. (2000) The PAS superfamily: Sensors of environmental and developmental signals. *Annu. Rev. Pharmacol. Toxicol. 40*, 519–561.

(6) Denison, M. S., and Heath-Pagliuso, S. (1998) The Ah receptor: A regulator of the biochemical and toxicological actions of structurally diverse chemicals. *Bull. Environ. Contam. Toxicol. 61*, 557–568.

(7) Poland, A., and Knutson, J. C. (1982) 2,3,7,8-tetrachlorodibenzo-p-dioxin and related halogenated aromatic hydrocarbons: Examination

of the mechanism of toxicity. *Annu. Rev. Pharmacol. Toxicol. 22*, 517–554.

(8) Hankinson, O. (1995) The aryl hydrocarbon receptor complex. *Annu. Rev. Pharmacol. Toxicol. 35*, 307–340.

(9) Swanson, H., Chan, W., and Bradfield, C. (1995) DNA binding specificities and pairing rules of the Ah receptor, ARNT, and SIM proteins. *J. Biol. Chem. 270*, 26292–26302.

(10) Gillesby, B. E., Stanostefano, M., Porter, W., Safe, S., Wu, Z. F., and Zacharewski, T. R. (1997) Identification of a motif within the 5′ regulatory region of pS2 which is responsible for AP-1 binding and TCDD-mediated suppression. *Biochemistry 36*, 6080–6089.

(11) Lusska, A., Shen, E., and Whitlock, J. P. (1993) Protein-DNA interactions at a dioxin-responsive enhancer. Analysis of six bona fide DNA-binding sites for the liganded Ah receptor. *J. Biol. Chem. 268*, 6575–6580.

(12) Shen, E. S., and Whitlock, J. P. (1992) Protein-DNA interactions at a dioxin-responsive enhancer. Mutational analysis of the DNA-binding site for the liganded Ah receptor. *J. Biol. Chem. 267*, 6815–6819.

(13) Quandt, K., Frech, K., Karas, H., Wingender, E., and Werner, T. (1995) MatInd and MatInspector: New fast and versatile tools for detection of consensus matches in nucleotide sequence data. *Nucleic Acids Res. 23*, 4878–4884.

(14) Sun, Y. V., Boverhof, D. R., Burgoon, L. D., Fielden, M. R., and Zacharewski, T. R. (2004) Comparative analysis of dioxin response elements in human, mouse and rat genomic sequences. *Nucleic Acids Res. 32*, 4512–4523.

(15) Church, D. M., Goodstadt, L., Hillier, L. W., Zody, M. C., Goldstein, S., She, X., Bult, C. J., Agarwala, R., Cherry, J. L., DiCuccio, M., Hlavina, W., Kapustin, Y., Meric, P., Maglott, D., Birtle, Z., Marques, A. C., Graves, T., Zhou, S., Teague, B., Potamousis, K., Churas, C., Place, M., Herschleb, J., Runnheim, R., Forrest, D., Amos-Landgraf, J., Schwartz, D. C., Cheng, Z., Lindblad-Toh, K., Eichler, E. E., Ponting, C. P., and Consortium, M. G. S. (2009) Lineage-specific biology revealed by a finished genome assembly of the mouse. *PLoS Biol. 7*, e1000112.

(16) Worley, K. C., Weinstock, G. M., and Gibbs, R. A. (2008) Rats in the genomic era. *Physiol. Genomics 32*, 273–282.

(17) Zody, M. C., Jiang, Z., Fung, H.-C., Antonacci, F., Hillier, L. W., Cardone, M. F., Graves, T. A., Kidd, J. M., Cheng, Z., Abouelleil, A., Chen, L., Wallis, J., Glasscock, J., Wilson, R. K., Reily, A. D., Duckworth, J., Ventura, M., Hardy, J., Warren, W. C., and Eichler, E. E. (2008) Evolutionary toggling of the MAPT 17q21.31 inversion region. *Nat. Genet. 40*, 1076–1083.

(18) Emi, Y., Ikushiro, S., and Iyanagi, T. (1996) Xenobiotic responsive element-mediated transcriptional activation in the UDP-glucuronosyltransferase family 1 gene complex. *J. Biol. Chem. 271*, 3952–3958.

(19) Favreau, L., and Pickett, C. (1991) Transcriptional regulation of the rat NAD(P)H:quinone reductase gene. Identification of regulatory elements controlling basal level expression and inducible expression by planar aromatic compounds and phenolic antioxidants. *J. Biol. Chem. 266*, 4556–4561.

(20) Fujisawa-Sehara, A., Sogawa, K., Yamane, M., and Fujii-Kuriyama, Y. (1987) Characterization of xenobiotic responsive elements upstream from the drug-metabolizing cytochrome P-450c gene: A similarity to glucocorticoid regulatory elements. *Nucleic Acids Res. 15*, 4179–4191.

(21) Pimental, R. A., Liang, B., Yee, G. K., Wilhelmsson, A., Poellinger, L., and Paulson, K. E. (1993) Dioxin receptor and C/EBP regulate the function of the glutathione S-transferase Ya gene xenobiotic response element. *Mol. Cell. Biol. 13*, 4365–4373.

(22) Yoo, H. Y., Chang, M. S., and Rho, H. M. (1999) Xenobiotic-responsive element for the transcriptional activation of the rat Cu/Zn superoxide dismutase gene. *Biochem. Biophys. Res. Commun. 256*, 133–137.

(23) Zhang, L., Savas, U., Alexander, D. L., and Jefcoate, C. R. (1998) Characterization of the mouse Cyp1B1 gene. Identification of an enhancer region that directs aryl hydrocarbon receptor-mediated constitutive and induced expression. *J. Biol. Chem. 273*, 5174–5183.

(24) Reisdorph, R., and Lindahl, R. (2007) Constitutive and 3-methylcholanthrene-induced rat ALDH3A1 expression is mediated by multiple xenobiotic response elements. *Drug Metab. Dispos. 35*, 386–393.

(25) Rhead, B., Karolchik, D., Kuhn, R., Hinrichs, A., Zweig, A., Fujita, P., Diekhans, M., Smith, K., Rosenbloom, K., Raney, B., Pohl, A., Pheasant, M., Meyer, L., Learned, K., Hsu, F., Hillman-Jackson, J., Harte, R., Giardine, B., Dreszer, T., Clawson, H., Barber, G., Haussler, D., and Kent, W. (2010) The UCSC Genome Browser database: update 2010. *Nucleic Acids Res. 38*, D613.

(26) Boverhof, D. R., Burgoon, L. D., Tashiro, C., Chittim, B., Harkema, J. R., Jump, D. B., and Zacharewski, T. R. (2005) Temporal and dose-dependent hepatic gene expression patterns in mice provide new insights into TCDD-Mediated hepatotoxicity. *Toxicol. Sci. 85*, 1048–1063.

(27) Eckel, J., Gennings, C., Therneau, T., Burgoon, L., Boverhof, D., and Zacharewski, T. (2005) Normalization of two-channel microarray experiments: A semiparametric approach. *Bioinformatics 21*, 1078–1083.

(28) Eckel, J., Gennings, C., Chinchilli, V., Burgoon, L., and Zacharewski, T. (2004) Empirical bayes gene screening tool for time-course or dose-response microarray data. *J. Biopharm. Stat. 14*, 647–670.

(29) Murray, I. A., Morales, J. L., Flaveny, C. A., Dinatale, B. C., Chiaro, C., Gowdahalli, K., Amin, S., and Perdew, G. H. (2010) Evidence for ligand-mediated selective modulation of aryl hydrocarbon receptor activity. *Mol. Pharmacol. 77*, 247–254.

(30) Boutros, P. C., Yan, R., Moffat, I. D., Pohjanvirta, R., and Okey, A. B. (2008) Transcriptomic responses to 2,3,7,8-tetrachlorodibenzo-p-dioxin (TCDD) in liver: Comparison of rat and mouse. *BMC Genomics 9*, 419.

(31) Boverhof, D. R., Burgoon, L. D., Tashiro, C., Sharratt, B., Chittim, B., Harkema, J. R., Mendrick, D. L., and Zacharewski, T. R. (2006) Comparative toxicogenomic analysis of the hepatotoxic effects of TCDD in Sprague Dawley rats and C57BL/6 mice. *Toxicol. Sci. 94*, 398–416.

(32) Fletcher, N., Wahlström, D., Lundberg, R., Nilsson, C. B., Nilsson, K. C., Stockling, K., Hellmold, H., and Håkansson, H. (2005) 2,3,7,8-Tetrachlorodibenzo-p-dioxin (TCDD) alters the mRNA expression of critical genes associated with cholesterol metabolism, bile acid biosynthesis, and bile transport in rat liver: A microarray study. *Toxicol. Appl. Pharmacol. 207*, 1–24.

(33) Hayes, K., Zastrow, G., Nukaya, M., Pande, K., Glover, E., Maufort, J., Liss, A., Liu, Y., Moran, S., Vollrath, A., and Bradfield, C. (2007) Hepatic transcriptional networks induced by exposure to 2,3,7,8-tetrachlorodibenzo-p-dioxin. *Chem. Res. Toxicol. 20*, 1573–1581.

(34) Puga, A., Maier, A., and Medvedovic, M. (2000) The transcriptional signature of dioxin in human hepatoma HepG2 cells. *Biochem. Pharmacol. 60*, 1129–1142.

(35) Tijet, N., Boutros, P. C., Moffat, I. D., Okey, A. B., Tuomisto, J., and Pohjanvirta, R. (2006) Aryl hydrocarbon receptor regulates distinct dioxin-dependent and dioxin-independent gene batteries. *Mol. Pharmacol. 69*, 140–153.

(36) Ovando, B. J., Vezina, C. M., McGarrigle, B. P., and Olson, J. R. (2006) Hepatic gene downregulation following acute and subchronic exposure to 2,3,7,8-tetrachlorodibenzo-p-dioxin. *Toxicol. Sci. 94*, 428–438.

(37) Yauk, C. L., Jackson, K., Malowany, M., and Williams, A. (2010) Lack of change in microRNA expression in adult mouse liver following treatment with benzo(a)pyrene despite robust mRNA transcriptional response. *Mutat. Res.* In press.

(38) Bourdeau, V., Deschênes, J., Métivier, R., Nagai, Y., Nguyen, D., Bretschneider, N., Gannon, F., White, J. H., and Mader, S. (2004) Genome-wide identification of high-affinity estrogen response elements in human and mouse. *Mol. Endocrinol. 18*, 1411–1427.

(39) Lemay, D. G., and Hwang, D. H. (2006) Genome-wide identification of peroxisome proliferator response elements using integrated computational genomics. *J. Lipid Res. 47*, 1583–1587.

(40) Menendez, D., Inga, A., and Resnick, M. A. (2010) Estrogen receptor acting in cis enhances WT and mutant p53 transactivation at

canonical and noncanonical p53 target sequences. *Proc. Natl. Acad. Sci. U.S.A. 107*, 1500–1505.

(41) Nukaya, M., Moran, S., and Bradfield, C. A. (2009) The role of the dioxin-responsive element cluster between the Cyp1a1 and Cyp1a2 loci in aryl hydrocarbon receptor biology. *Proc. Natl. Acad. Sci. U.S.A. 106*, 4923–4928.

(42) Ortiz-Barahona, A., Villar, D., Pescador, N., Amigo, J., and Del Peso, L. (2010) Genome-wide identification of hypoxia-inducible factor binding sites and target genes by a probabilistic model integrating transcription-profiling data and in silico binding site prediction. *Nucleic Acids Res. 38*, 2332–2345.

(43) van Batenburg, M. F., Li, H., Polman, J. A., Lachize, S., Datson, N. A., Bussemaker, H. J., and Meijer, O. C. (2010) Paired hormone response elements predict caveolin-1 as a glucocorticoid target gene. *PLoS ONE 5*, e8839.

(44) Xue, Y., Sun, D., Daly, A., Yang, F., Zhou, X., Zhao, M., Huang, N., Zerjal, T., Lee, C., Carter, N. P., Hurles, M. E., and Tyler-Smith, C. (2008) Adaptive evolution of UGT2B17 copy-number variation. *Am. J. Hum. Genet. 83*, 337–346.

(45) Farnham, P. J. (2009) Insights from genomic profiling of transcription factors. *Nat. Rev. Genet. 10*, 605–616.

(46) Li, Q., Barkess, G., and Qian, H. (2006) Chromatin looping and the probability of transcription. *Trends Genet. 22*, 197–202.

(47) Long, X., and Miano, J. M. (2007) Remote control of gene expression. *J. Biol. Chem. 282*, 15941–15945.

(48) Silkworth, J. B., Carlson, E. A., McCulloch, C., Illouz, K., Goodwin, S., and Sutter, T. R. (2008) Toxicogenomic analysis of gender, chemical, and dose effects in livers of TCDD- or aroclor 1254-exposed rats using a multifactor linear model. *Toxicol. Sci. 102*, 291–309.

(49) Walker, N. J., Wyde, M. E., Fischer, L. J., Nyska, A., and Bucher, J. R. (2006) Comparison of chronic toxicity and carcinogenicity of 2,3,7,8-tetrachlorodibenzo-p-dioxin (TCDD) in 2-year bioassays in female Sprague-Dawley rats. *Mol. Nutr. Food Res. 50*, 934–944.

(50) Twigger, S. N., Pruitt, K. D., Fernández-Suárez, X. M., Karolchik, D., Worley, K. C., Maglott, D. R., Brown, G., Weinstock, G., Gibbs, R. A., Kent, J., Birney, E., and Jacob, H. J. (2008) What everybody should know about the rat genome and its online resources. *Nat. Genet. 40*, 523–527.

(51) Saxonov, S., Berg, P., and Brutlag, D. L. (2006) A genome-wide analysis of CpG dinucleotides in the human genome distinguishes two distinct classes of promoters. *Proc. Natl. Acad. Sci. U.S.A. 103*, 1412–1417.

(52) Nakajima, M., Iwanari, M., and Yokoi, T. (2003) Effects of histone deacetylation and DNA methylation on the constitutive and TCDD-inducible expressions of the human CYP1 family in MCF-7 and HeLa cells. *Toxicol. Lett. 144*, 247–256.

(53) Badis, G., Berger, M. F., Philippakis, A. A., Talukder, S., Gehrke, A. R., Jaeger, S. A., Chan, E. T., Metzler, G., Vedenko, A., Chen, X., Kuznetsov, H., Wang, C.-F., Coburn, D., Newburger, D. E., Morris, Q., Hughes, T. R., and Bulyk, M. L. (2009) Diversity and complexity in DNA recognition by transcription factors. *Science 324*, 1720–1723.

(54) Jaeger, S. A., Chan, E. T., Berger, M. F., Stottmann, R., Hughes, T. R., and Bulyk, M. L. (2010) Conservation and regulatory associations of a wide affinity range of mouse transcription factor binding sites. *Genomics 95*, 185–195.

(55) Cicatiello, L., Addeo, R., Sasso, A., Altucci, L., Petrizzi, V. B., Borgo, R., Cancemi, M., Caporali, S., Caristi, S., Scafoglio, C., Teti, D., Bresciani, F., Perillo, B., and Weisz, A. (2004) Estrogens and progesterone promote persistent CCND1 gene activation during G1 by inducing transcriptional derepression via c-Jun/c-Fos/estrogen receptor (progesterone receptor) complex assembly to a distal regulatory element and recruitment of cyclin D1 to its own gene promoter. *Mol. Cell. Biol. 24*, 7260–7274.

(56) Owen, G. I., Richer, J. K., Tung, L., Takimoto, G., and Horwitz, K. B. (1998) Progesterone regulates transcription of the p21(WAF1) cyclin- dependent kinase inhibitor gene through Sp1 and CBP/p300. *J. Biol. Chem. 273*, 10696–10701.

(57) Stoecklin, E., Wissler, M., Schaetzle, D., Pfitzner, E., and Groner, B. (1999) Interactions in the transcriptional regulation exerted by Stat5 and by members of the steroid hormone receptor family. *J. Steroid Biochem. Mol. Biol. 69*, 195–204.

(58) Ahmed, S., Valen, E., Sandelin, A., and Matthews, J. (2009) Dioxin increases the interaction between aryl hydrocarbon receptor and estrogen receptor alpha at human promoters. *Toxicol. Sci. 111*, 254–266.

(59) Beischlag, T. V., and Perdew, G. H. (2005) ER alpha-AHR-ARNT protein-protein interactions mediate estradiol-dependent transrepression of dioxin-inducible gene transcription. *J. Biol. Chem. 280*, 21607–21611.

(60) Boutros, P. C., Moffat, I. D., Franc, M. A., Tijet, N., Tuomisto, J., Pohjanvirta, R., and Okey, A. B. (2004) Dioxin-responsive AHRE-II gene battery: Identification by phylogenetic footprinting. *Biochem. Biophys. Res. Commun. 321*, 707–715.

(61) Sogawa, K., Numayama-Tsuruta, K., Takahashi, T., Matsushita, N., Miura, C., Nikawa, J.-i., Gotoh, O., Kikuchi, Y., and Fujii-Kuriyama, Y. (2004) A novel induction mechanism of the rat CYP1A2 gene mediated by Ah receptor-Arnt heterodimer. *Biochem. Biophys. Res. Commun. 318*, 746–755.